Addition of $Sm_{0.2}Ce_{0.8}O_{1.9}$ Carbonate into Perovskite Cathode Materials for Low-Temperature Solid Oxide Fuel cell: Short Review

Tan Kang Huai[1*], Hamimah Binti Abd.Rahman[2], Muhammad Izzat Nor Ma'arof [1]
[1] INTI International University, Persiaran Perdana BBN, Putra Nilai, 71800, Nilai, Negeri Sembilan
[2] Universiti Tun Hussein Onn Malaysia, Parit Raja, 86400, Batu Pahat, Johor

[*]**Email**: kanghuai.tan@newinti.edu.my

Received*:15 December 2021;* ***Accepted****:23 January 2022;* ***Published****:25 January 2022*

Abstract: Solid Oxide Fuel Cells (SOFCs) are considered one of the most efficient energy conversion devices to meet sustainable and environmental energy resources. The high operating temperature (>800^{o}C) of SOFCs restrains the fabrication cost, material selection, and long-term material durability. Therefore, those cons of HT-SOFC have initiated the efforts of lowering down the SOFCs operating temperature. This article extensively reviews the materials development in low-temperature solid oxide fuel cells (LT-SOFC) (<600^{o}C). $Sm_{0.2}Ce_{0.8}O_{1.9}$ carbonate (SDCC) is developed and proved to facilitate ions transportation and low ohmic resistance at low-temperature operation compared to SDC and others electrolyte materials. The composition of carbon and calcination temperature in fabricating SDCC exhibit varying effects on the SDCC characterization and performance. Conventional perovskite materials such as $La_{0.6}Sr_{0.4}Co_{0.2}Fe_{0.8}O_{3-\alpha}$ (LSCF), $Ba_{0.5}Sr_{0.5}Co_{0.8}Fe_{0.2}O_{3-\alpha}$ (BSCF) and $Sm_{0.5}Sr_{0.5}Co_{8}O_{3-\alpha}$ (SSC) are incorporated with SDCC electrolyte materials in the application of the cathode and interconnect coatings as well. The SDCC incorporation in the LSCF perovskite produces excellent power output and low polarization resistance in low temperatures. The incorporation of SDCC into SSC requires further investigation due to the formation of $SrCO_3$ impurity. Besides, BSCF-SDCC perovskite exhibits better material characteristics with no calcination process involved. BSCF-SDCC attains low area-specific resistance.

Keywords: Solid oxide fuel cell; Perovskite Cathode; SDCC electrolyte; Low temperature

1.Introduction

Today, most of the global energy supply still relies on fossil fuels such as charcoal, petroleum, and etc. Major emissions of carbon compound gas from fossil fuel combustion led to the depletion of the earth's ozone layer and global warming (Nyarko et al., 2021). It is vital to look for alternative green energy sources to reduce environmental contamination and the greenhouse effect. Solid oxide fuel cells (SOFC) stand out on account of several green energy resources such as having high-energy conversion efficiency, fuel flexibility, broad range of power density and insignificant greenhouse gas emissions (Singh et al., 2021)

A single SOFC fuel cell consists of two porous electrodes of an anode and a cathode sandwiching a dense solid oxide electrolyte that is not permeable to other ions, as shown in Figure 1 (Hussain et al., 2020). Interconnect layer is the current collector integrated on top of each electrode. It also transports the electricity to the external circuit. The cathode is in contact with the oxidant, where oxygen is reduced into O^{2-} ions. The O^{2-} ions travel through the dense electrolyte into the anode to oxidize hydrogen gas into the water, releasing electrons into interconnect and brings back to the cathode.

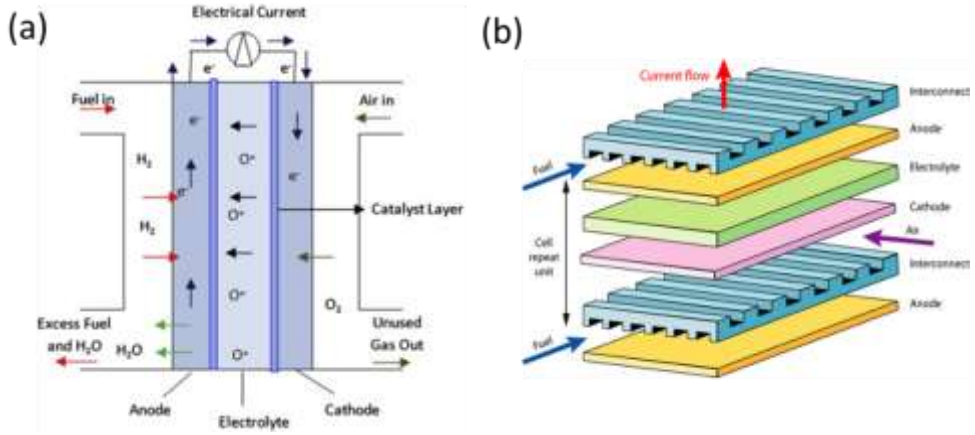

Figure 1. (a)Schematic diagram of solid oxide fuel cell working principle (b) Interconnect sandwiches a single SOFC (Tan et al., 2021)

In SOFC, perovskite cathode has been investigated widely as many metal oxides are susceptible to air environments in high temperatures (Rehman et al., 2019). Conventional SOFC operates at very high temperatures over 800^{o}C to excite oxygen catalytic activity and electric conductivity in perovskite materials. However, SOFC components in excessive high-temperature encounter materials degradation, short lifetime, long start-up time, lower thermal and redox cycle material stresses, restriction of material selection and high manufacturing cost for sustainability factor (Kumar Sharma et al., 2019). $La_{0.8}Sr_{0.2}MnO_{3-\delta}$ (LSM), $La_{0.6}Sr_{0.4}Co_{0.2}Fe_{0.8}O_{3-\alpha}$ (LSCF), $Ba_{0.5}Sr_{0.5}Co_{0.8}Fe_{0.2}O_{3-\alpha}$ (BSCF) and $Sm_{0.5}Sr_{0.5}Co_{8}O_{3-\alpha}$ (SSC) are perovskite cathode materials which persist high electric conductivity at high temperature (Bu et al, 2016). High polarization resistance and low electric conductivity are presented when it is brought to low temperature (Yang et al., 2021).

Several approaches are pioneered to develop and implement novel materials with enhanced oxygen-ion conductivity and electrode catalytic activities at low temperatures. However, materials remain incapable of achieving good cell resistance at low temperatures due to their low stability and low catalytic activity. Employing thin-film and microfabrication processes has been struggled by reducing the electrolyte thickness and increasing the reaction surface (Noh et al., 2014). However, major of these attempts are still appointed low electrochemical performance and cell scalability. In another investigation points, $Sm_{0.2}Ce_{0.8}O_{1.9}$ carbonate (SDCC) is developed as a low-temperature SOFC electrolyte (Ali et al., 2013). It achieves low polarization resistance and proves to facilitate ion conductivity. SDCC is also incorporated into conventional perovskite materials, and the findings contribute promising materials characterization and electrochemical properties. In this paper, the SDCC electrolyte's development and perovskites-SDCC materials are reviewed.

2. Development of $Sm_{0.2}Ce_{0.8}O_{1.9}$ carbonate (SDCC)

General electrolytes that are applied in high-temperature SOFC are $Sm_{0.2}Ce_{0.8}O_{1.9}$ (SDC) and $Ce_{0.9}Gd_{0.1}O_{1.9}$ (GDC). Increasing ionic conductivity at low-temperature SOFC can be accomplished by doping a small amount of alkaline salt carbonates into ceria-based electrolytes. Lithium (Li), sodium (Na), or potassium (K) is an alkaline metal that incorporates into carbonates. Various alkaline metals combinations were experimented in order to examine their relation with ionic conductivity (Huang, Gao and Mao, 2010). The result has shown that a combination of (Li, Na)CO_3 exhibiting better conductivity from 400ºC to 600ºC. This result is similar to Boden et al. (2007), which stated that (Li,Na)CO_3 manifests better conductivity and low activation energy at low-temperature SOFC.

Generally, the dual doped ceria composites such as SDCC and GDCC have higher ionic conductivity than corresponding single-phase doped ceria materials in LT-SOFC. Among all the (Li, Na)CO_3 carbonate composite electrolyte, SDCC exhibits the excellent impedance characteristic with excellent ionic conductivity of 0.08 S/cm at a maximum of 650ºC which is much higher than pure SDC and GDC as shown in Figure 2(Ali et al., 2015). SDCC electrolyte produces hybrid ionic conduction of O^{2-} from oxygen vacancy of ceria lattice and H^+ from temporal bonding with CO_3^{2-}. This carbonate assists the transfer of both ions by providing path and transportation at the interfaces of two two-phase materials, and the conduction process is shown in Figure 3.0. It leads to excellent conduction that enhances electrolyte performance (Fan et al., 2013).

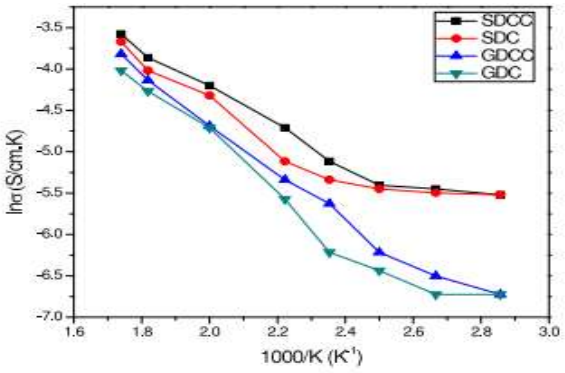

Figure 2. Ionic Conductivity between SDCC, SDC , GDCC and GDC (Ali *et al*, 2015)

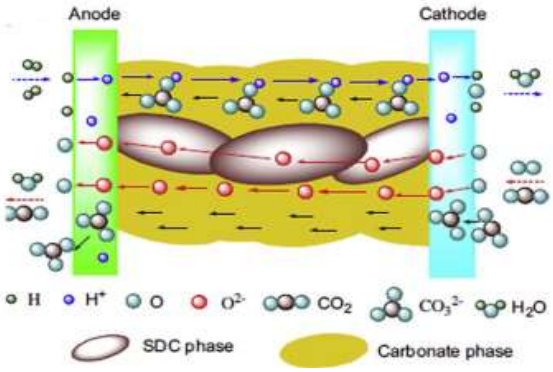

Figure 3. Electrolyte interfacial conduction mechanism (Fan *et al.*, 2013)

Ali et al. (2015) fabricated the SDCC electrolyte powder with 20 wt% (Li/Na)CO_3 followed by 680ºC calcination temperature. The SDCC powder is cold-pressed into pellets and sintered under 500ºC to 650ºC. The samples are undergone microstructure analysis and impedance testing operating at 500ºC and 550ºC. The 500SDCC showed inadequate melting of carbonates while 550SDCC showed no interface between SDCC and (Li/ Na)CO_3 phases with no clear pores, as shown in Figure 4(a). However, the 600SDCC and 650SDCC exhibit non-continuous phases as shown in Figure 4 (b). Figure 5 indicates the electrochemical impedance spectroscopy (EIS) Nyquist plot. The arc of SDCC composite becomes smaller with the decrease in sintering temperature. 550SDCC shows the most minor arc operating at 550ºC, representing 0.077 S/cm, which improved from the previous readings.

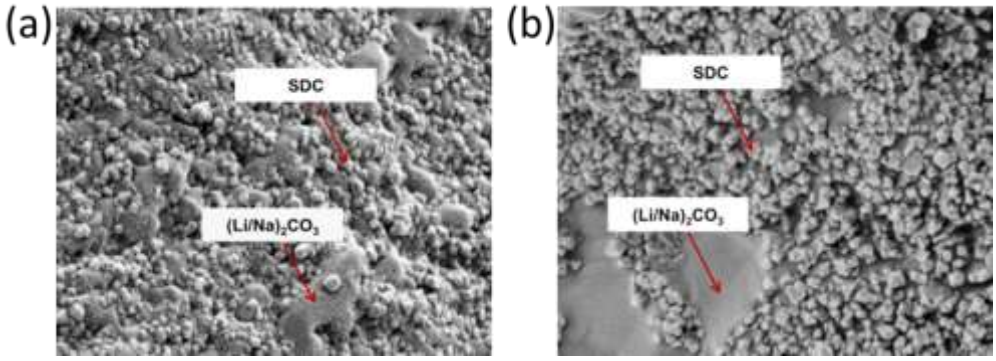

Figure 4. SEM image of (a) 550 SDCC and (b) 650 SDCC electrolyte (Ali et al., 2015)

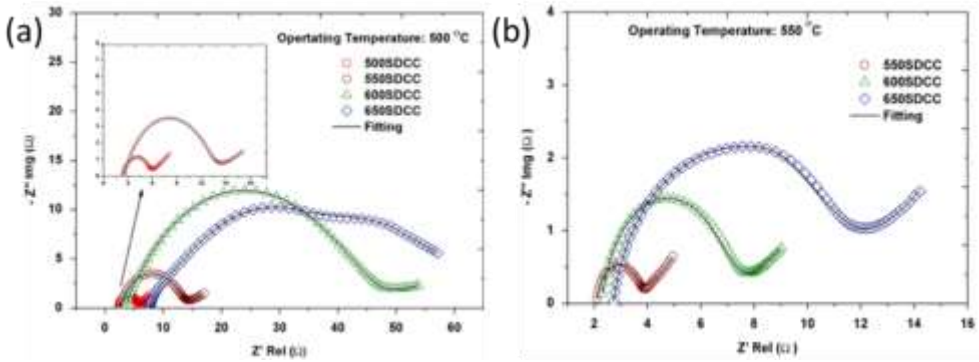

Figure 5. EIS plot for the sintered SDCC at 500ºC and 550ºC operating temperature (Ali et al., 2015)

3. Incorporating SDCC into $La_{0.6}Sr_{0.4}Co_{0.2}Fe_{0.8}O_{3-\alpha}$ (LSCF)

Incorporating SDCC electrolyte into perovskite materials LSCF, SSC, BSCF are initiated by ball milling technique. The ball milling method effectively reduces particle size for uniform distribution mixing of the particles (Cho & Choi, 2008; Sopicka-Lizer, 2010). The rotational speed of the milling process is essential to prepare nanomaterials, various types of nanocomposites. Rahman et al. (2013) fabricate LSCF-SDCC mixing with 30-50wt%SDCC by 550 rpm ball milling. The dried powder was calcined from 750 to 850ºC and followed cold-pressed into pellet form. The trend of the thermal expansion coefficient (TEC) result demonstrates that an increase SDCC electrolyte amount in the composite cathode LSCF-SDCC brings the TEC of the cathode closer to the electrolyte. The TEC of SDCC electrolyte is 3.36 x 10^{-6} K^{-1}. The TEC of LSCF-SDCC55 (calcined from 750-900ºC) shows TEC values from 3.13-3.66 x 10^{-6} K^{-1}, 3.81-6.15 x 10^{-6} K^{-1} for LSCF-SDCC64 and 4.59- 5.84 x 10-6 K^{-1}. Matched TEC between electrodes could reduce spallation occurring due to the thermal stress exerted between the components in SOFC. The reported phase crystallinity of LSCF and SDCC in LSCF-SDCC is good without any distortion of secondary phases.

The particle size of the LSCF-SDCC55 increases gradually when the calcination temperature increases, as shown in Figure 6 below. According to the theory of calcination in ceramic materials, thermal treatment increases powder particle size while decreases surface area. A better-equiaxed shape of particles is obtained when calcination temperature increases. The

author also investigates the power density of a single cell with NiO-SDCC as anode and SDCC as electrolyte with constant parameters. The study finds out that the power output of LSCF-SDCC55 calcined 700ºC is 120.4 mW cm^{-2} at 550ºC operating temperature, power output of LSCF-SDCC55 calcined 750ºC and 800ºC are 117.9 mW cm^{-2} and 71.8 mW cm^{-2}. Ali et al. (2020) also investigated the effect of low calcination temperature (600ºC) towards LSCF-SDCC55. However, the lower calcination temperature of LSCF-SDCC55 attributes to lower power density. The power density achieves approximately 70 mW cm^{-2} for all operating temperatures of LSCF-SDCC calcined at 600ºC as shown in Figure 7. It concludes that from the calcination temperature, 600ºC to 900ºC, the 700ºC exhibits better materials characterization and power performance. This is because the lower the particle size, the higher the surface areas of the powders. Thus, it increases the triple-phase boundary (TPB) within the electrode for a higher catalytic reaction, and the TPB increase enhanced the cell performance (Timurkutluk et al., 2021). Rahman et al. (2019) investigate the similar study with the effect of calcination temperature from 700ºC to 900ºC. It indicates that low polarization resistance is achieved by LSCF-SDCC55 with ASR value from 0.35 to 0.54 Ωcm^2 at operating temperature 475–550°C.

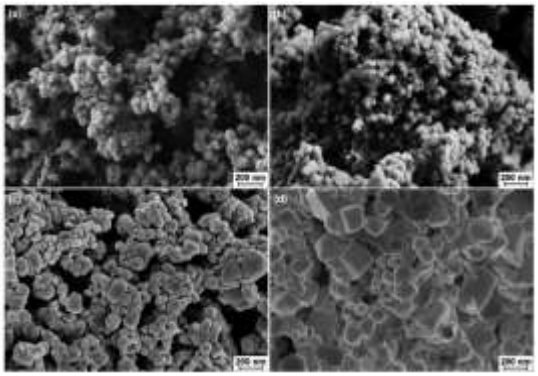

Figure 6. FESEM micrographs of LSCF-SDCC55 powder calcined at (a) 750ºC (b)800ºC (c)850ºC and (d) 900ºC (Rahman et al., 2013)

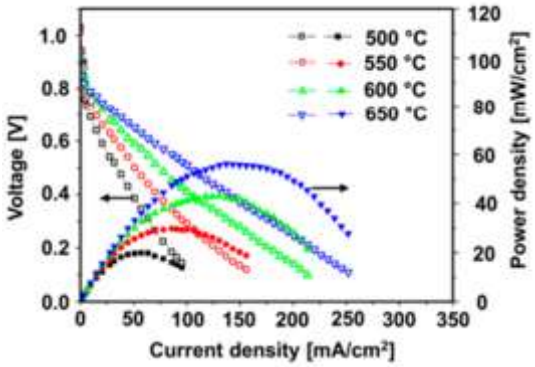

Figure 7. Performance of single cell operates at 500-650ºC for LSCF-SDCC66 calcined 600ºC (Ali et al., 2020)

4. Incorporating SDCC into $Sm_{0.5}Sr_{0.5}Co_8O_{3-\alpha}$ (SSC)

$Sm_{0.5}Sr_{0.5}Co_8O_{3-\alpha}$ is revealed as a potential cathode material because of its higher electric conductivity than LSCF and BSCF. However, research indicates impurities or secondary phases

from SSC such as strontium carbonate (strontianite), $SrCO_3$, and strontium cobalt carbonate $SrCoCO_3$ prompt structural instability (Mohammad et al., 2019). This has restrained the SSC performance durability and sustainability. This section reviews the material's physical characterization after incorporating SDCC into SSC. Mohamed conducts the X-ray diffraction (XRD) of SSC-SDCC with various compositions of SDCC. As shown in Figure 5, XRD diffractogram reveals the formation of $SrCO_3$ after calcination. The construction of $SrCO_3$ increased when the calcination temperature increases. This might be due to the carbonate layer in the SSC-SDCC, which prompts the reaction between Sr atom and the carbonate layer. This is supported by Yang et al. (2017) that when SSC calcination temperature increases, the CO_2 in the air reacts with Sr to produce $SrCO_3$ impurity. The smaller atomic size of Sr prompts to evacuate from A site perovskite structure compared to LSCF and BSCF. La and Ba exhibit a larger atomic size, which reduces the opportunity of Sr to evacuate out of the structure. The extensive studies need to be conducted on SSC perovskite to inhibit the formation $SrCO_3$ as potential cathode candidates in SOFC.

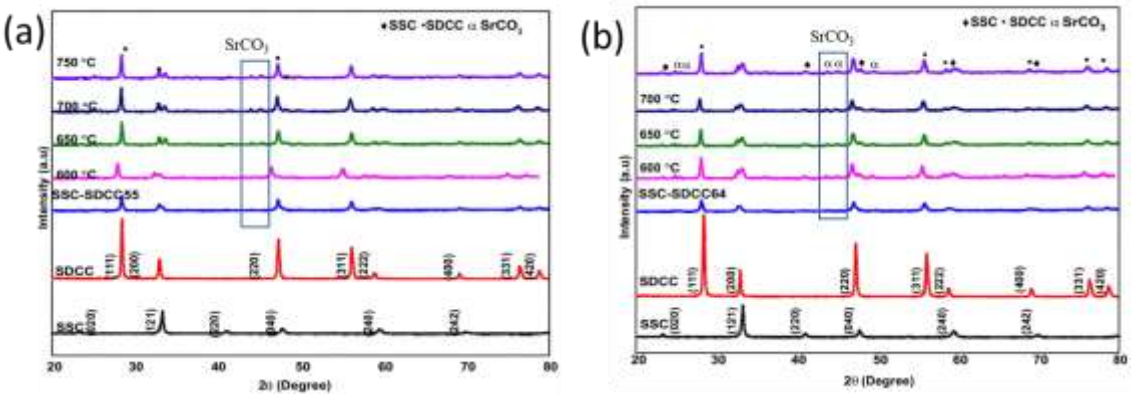

Figure 8. XRD diffractograms for calcined (a) SSC-SDCC55 and (b) SSC-SDCC64 (Mohammad et al., 2019)

5. Incorporating SDCC into $Ba_{0.5}Sr_{0.5}Co_{0.8}Fe_{0.2}O_{3-\alpha}$ (BSCF)

$Ba_{0.5}Sr_{0.5}Co_{0.8}Fe_{0.2}O_{3-\alpha}$ is developed by substituting Ba from La into A site perovskite structure of LSCF to analyse its properties in low-temperature SOFC. Despite low electric conductivity achieved in low-temperature operation compared to LSCF and SSC, the polarization resistance of BSCF is the lowest among perovskite materials (Shen & Lu, 2016). This implies that with the existence of Ba in perovskite, the oxygen is efficiently catalysed into ions. However, the low electric conductivity at a low temperature represents that the ionic conduction in BSCF is slow. Research effort on increasing ionic conductivity in BSCF at low temperatures is essential. Incorporating SDCC into BSCF has been started recently. Linda et al. (2016) have initiated mixing BSCF-SDCC by ratio 50:50 wt% (BSCF-SDCC55) in high-speed ball milling technique. Appropriate particle size, particle micrograph, porosity and elemental distribution are achieved. The research effort is continued by Tan et al. (2018) by mixing various milling speeds. The findings show that the BSCF's crystalline phase intensity is decreased when the milling speed is increased to 200 rpm, as shown in Figure 9 (a). Furthermore, the BSCF crystalline phase in BSCF-SDCC is destructed when only a low calcination temperature is applied as shown in Figure 9 (b). The formation of $BaCO_3$ is observed which could literally decrease the SOFC performance, according to Qiu et al. (2017). Therefore, fabricating BSCF-SDCC is achieved in low milling

speed without calcination. This is supported by Ng et al. (2017) that calcination promotes the formation of $BaCO_3$ until calcination temperature reaches 900°C. This is enough temperature to remove $BaCO_3$ impurity and heal the BSCF crystallinity.

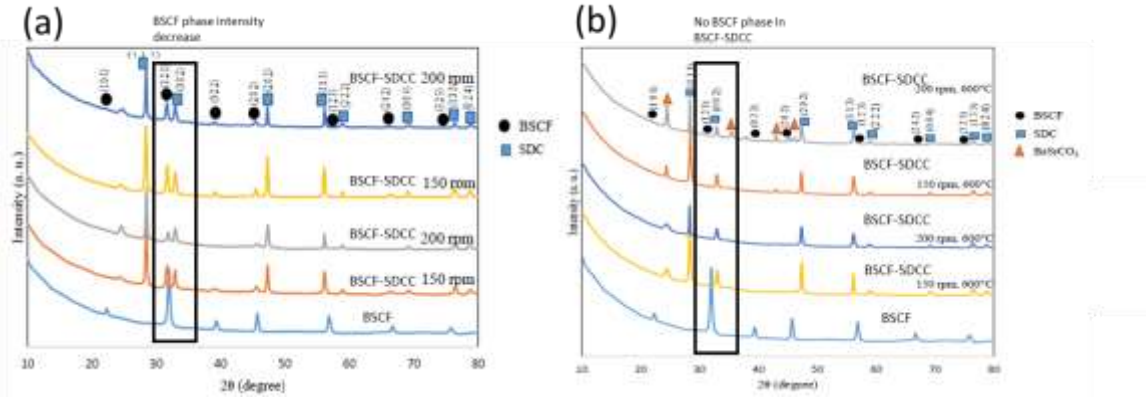

Figure 9.0. XRD diffractogram of BSCF-SDCC in different milling speed and calcination (Tan et al., 2018)

Up today, BSCF-SDCC is only applied in interconnect protective coatings to inhibit the growth of chromia scale, Cr_2O_3. The chromia scale is reported impeding the electron transfer in interconnect (Jia et al., 2019). This deteriorates the electric conductivity in SOFC performance. BSCF-SDCC is coated on interconnect as a barrier for Cr diffusion and migration of chromia sale to the cathode (Tan et al., 2020). BSCF-SDCC is sintered from 500-700°C after it is coated by the electrophoretic deposition method. The findings show that the coating sintered 600°C manifests uniform coating while coating sintered 700°C shows the existence of crack as shown in Figure 10.0. This might due to the thermal stress exerted in large temperature sintering between ferritic stainless-steel interconnect and the coating (Ebrahimifar et al., 2015). However, there is a clear formation of pores on the coating without sintering. Sintering is playing an essential role in facilitating the growth of the coating particles into a compact one (Abdoli et al., 2020). Calcination is not suitable for BSCF-SDCC powder as a secondary phase is formed (Tan et al., 2018). However, in BSCF-SDCC coating, sintering is proper as dense coating reduces the surface area for oxygen to diffuse into the coating. Plus, sintering assists in compacting the dense coating. The crystalline phase of BSCF in BSCF-SDCC sintered 600°C is still observed except for coating non-sintering and sintered 700°C, BSCF crystallinity is reduced. The ASR reports a reading of $0.073\Omega cm^2$ after 500 hour oxidation test is completed.

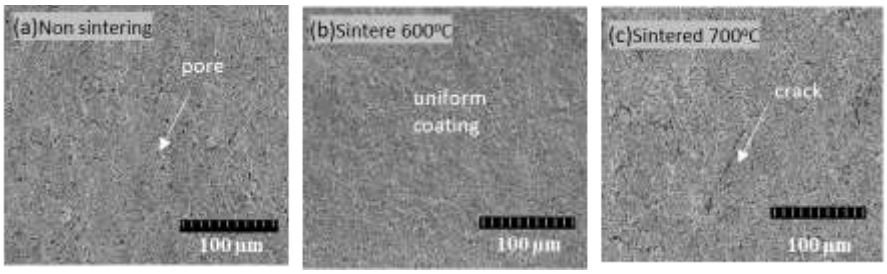

Figure 10. Coating surface of BSCF-SDCC in different sintering temperatures (Tan *et al*., 2020)

6. Conclusion

In conclusion, incorporating SDCC into perovskite materials is promising for low-temperature SOFC material development. Good material characterization such as particle crystallinity and microstructure are vital to achieve better SOFC performance. LSCF-SDCC perovskite is investigated in terms of cathode application, and excellent power density is achieved. SSC-SDCC is new developed perovskite material but further studies need to be done on crystallinity. BSCF-SDCC perovskite is successfully investigated and applied in interconnect coating. Uniform coating and low area specific resistance are achieved for the coating.

Acknowledgement

The authors would like to thank the INTI International University for supporting this research under INTI IU Research Seeding Grant 2021: INTI-FEQS-16-03-2021.

References

Abdoli, H., Molin, S., & Farnoush, H. (2020). Effect of interconnect coating procedure on solid oxide fuel cell performance. Materials Letters, 259, 126898.

Ali, S. M., Muchtar, A., Sulong, A. B., Muhamad, N., & Majlan, E. H. (2013). Influence of sintering temperature on the power density of samarium-doped-ceria carbonate electrolyte composites for low-temperature solid oxide fuel cells. Ceramics International, 39(5), 5813-5820.

Ali, S. M., Rosli, R. E., Muchtar, A., Sulong, A. B., Somalu, M. R., & Majlan, E. H. (2015). Effect of sintering temperature on surface morphology and electrical properties of samarium-doped ceria carbonate for solid oxide fuel cells. Ceramics International, 41(1), 1323-1332.

SA, M. A., Raharjo, J., Anwar, M., Khaerudini, D. S., Muchtar, A., Spiridigliozzi, L., & Somalu, M. R. (2020). Carbonate-Based Lanthanum Strontium Cobalt Ferrite (LSCF)–Samarium-Doped Ceria (SDC) Composite Cathode for Low-Temperature Solid Oxide Fuel Cells. Applied Sciences, 10(11), 3761.

Bodén, A., Di, J., Lagergren, C., Lindbergh, G., & Wang, C. Y. (2007). Conductivity of SDC and (Li/Na) 2CO3 composite electrolytes in reducing and oxidising atmospheres. Journal of Power Sources, 172(2), 520-529.

Bu, Y., Chen, Y., Wei, T., Lai, S., Ding, D., Sun, H., & Zhong, Q. (2016). Composites of single/double perovskites as cathodes for solid oxide fuel cells. Energy Technology, 4(7), 804-808.

Cho, H. J., & Choi, G. M. (2008). Effect of milling methods on performance of Ni–Y_2O_3-stabilized ZrO_2 anode for solid oxide fuel cell. Journal of Power Sources, 176(1), 96-101.

Ebrahimifar, H., & Zandrahimi, M. (2015). Oxidation and electrical behavior of a ferritic stainless steel with a Mn–Co-based coating for SOFC interconnect applications. Oxidation of metals, 84(3), 329-344.

Fan, L., Wang, C., Chen, M., & Zhu, B. (2013). Recent development of ceria-based (nano) composite materials for low temperature ceramic fuel cells and electrolyte-free fuel cells. Journal of Power Sources, 234, 154-174.

Huang, J., Gao, Z., & Mao, Z. (2010). Effects of salt composition on the electrical properties of samaria-doped ceria/carbonate composite electrolytes for low-temperature SOFCs. International journal of hydrogen energy, 35(9), 4270-4275.

Hussain, S., & Yangping, L. (2020). Review of solid oxide fuel cell materials: cathode, anode, and electrolyte. Energy Transitions, 1-14.

Jia, C., Wang, Y., Molin, S., Zhang, Y., Chen, M., & Han, M. (2019). High temperature oxidation behavior of SUS430 SOFC interconnects with Mn-Co spinel coating in air. Journal of Alloys and Compounds, 787, 1327-1335.

Kumar Sharma, D., Filipponi, M., Di Schino, A., Rossi, F., & Castaldi, J. (2019). Corrosion behaviour of high temperature fuel cells: Issues for materials selection. Metalurgija, 58(3-4), 347-351.

Agun, L., Ahmad Shah, M. H., Ahmad, S., & Rahman, H. A. (2016). $Ba_{0.5}Sr_{0.5}Co_{0.8}Fe_{0.2}$-SDC Carbonate Composite Cathode for Low-Temperature SOFCs. Materials Science Forum, 840, 247-251

Mohammad, S. F., Ahmad, S., Rahman, H. A., & Muchtar, A. (2019). Effect of SSC Loading on the Microstructural Stability SSC-SDCC Composite Cathode as New Potential SOFC. International Journal of Integrated Engineering, 11(7), 162-168.

Rahman, H. A., Ng, K. H., Ahmad, S., Taib, H., Mahzan, S., Salleh, S. M., . & Muchtar, A. (2019). Influence of microstructure on the electrochemical behaviour of LSCF-SDCC. In IOP Conference Series: Materials Science and Engineering 494(1), 012062.

Ng, K. H., Rahman, H. A., & Afandi, S. (2017). Effects of milling speed and calcination temperature on the phase stability of $Ba_{0.5}Sr_{0.5}Co_{0.8}Fe_{3-\delta}$. Materials Science Forum 888, 47-51

Noh, H. S., Yoon, K. J., Kim, B. K., Je, H. J., Lee, H. W., Lee, J. H., & Son, J. W. (2014). The potential and challenges of thin-film electrolyte and nanostructured electrode for yttria-stabilized zirconia-base anode-supported solid oxide fuel cells. Journal of Power Sources, 247, 105-111.

Nyarko, S. C., & Petcovic, H. L. (2021). Ghanaian preservice science teachers' knowledge of ozone depletion and climate change, and sources of their knowledge. International Journal of Science Education, 1-22.

Qiu, P., Yang, J., Jia, L., Gong, Y., Pu, J., & Li, J. (2017). Study on the ORR mechanism and CO2-poisoning resistance of La0. 8Sr0. 2MnO3-δ-coated $Ba_{0.5}Sr_{0.5}Co_{0.8}Fe_{0.2}O_{3-\delta}$ cathode for intermediate temperature solid oxide fuel cells. ECS Transactions, 78(1), 551.

Rahman, H. A., Muchtar, A., Muhamad, N., & Abdullah, H. (2013). $La_{0.6}Sr_{0.4}Co_{0.2}Fe_{0.8}O3- \delta-$ SDC carbonate composite cathodes for low-temperature solid oxide fuel cells. Materials Chemistry and Physics, 141(2-3), 752-757.

Rehman, A. U., Li, M., Knibbe, R., Khan, M. S., Peterson, V. K., Brand, H. E., & Zhu, Z. (2019). Enhancing oxygen reduction reaction activity and CO_2 tolerance of cathode for low-temperature solid oxide fuel cells by in situ formation of carbonates. ACS applied materials & interfaces, 11(30), 26909-26919.

Shen, F., & Lu, K. (2016). Perovskite-type $La_{0.6}Sr_{0.4}Co_{0.2}Fe_{0.8}O_3$, $Ba_{0.5}Sr_{0.5}Co_{0.2}Fe_{0.8}O_3$, and $Sm_{0.5}Sr_{0.5}Co_{0.2}Fe_{0.8}O_3$ cathode materials and their chromium poisoning for solid oxide fuel cells. Electrochimica Acta, 211, 445-452.

Singh, M., Zappa, D., & Comini, E. (2021). Solid oxide fuel cell: Decade of progress, future perspectives and challenges. International Journal of Hydrogen Energy, 46 (54), 27643-27674.

Sopicka-Lizer, M. (Ed.). (2010). High-energy ball milling: mechanochemical processing of nanopowders. Elsevier.

Tan, K. H., Rahman, H. A., Taib, H., Ahmad, S., Yusop, U. A., & Ibrahim, H. (2018). Influence of heat treatment and milling speed on phase stability of $Ba_{0.5}Sr_{0.5}Co_{0.8}Fe_{0.2}O_{3-\delta}$ composite cathode solid oxide fuel cell. Key Engineering Materials,791, 66-73.

Tan, K. H., Rahman, H. A., & Taib, H. (2019). Coating layer and influence of transition metal for ferritic stainless steel interconnector solid oxide fuel cell: A review. International Journal of Hydrogen Energy, 44(58), 30591-30605.

Tan, K. H., Rahman, H. A., & Taib, H. (2020). $Ba_{0.5}Sr_{0.5}Co_{0.8}Fe_{0.2}O_{3-\delta}$-$Sm_{0.2}Ce_{0.8}O_{1.9}$ carbonate perovskite coating on ferritic stainless steel interconnect for low temperature solid oxide fuel cells. Materials Chemistry and Physics, 254, 123433.

Timurkutluk, B., Altan, T., Toros, S., Genc, O., Celik, S., & Korkmaz, H. G. (2021). Engineering solid oxide fuel cell electrode microstructure by a micro-modeling tool based on estimation of TPB length. International Journal of Hydrogen Energy, 46(24), 13298-13317.

Yang, Z., Guo, M., Wang, N., Ma, C., Wang, J., & Han, M. (2017). A short review of cathode poisoning and corrosion in solid oxide fuel cell. International Journal of Hydrogen Energy, 42(39), 24948-24959.

Yang, D., Chen, G., Liu, H., Zhang, L., He, Y., Zhang, X., & Li, Y. (2021). Electrochemical performance of a $Ni_{0.8}Co_{0.15}Al_{0.05}LiO_2$ cathode for a low temperature solid oxide fuel cell. International Journal of Hydrogen Energy, 46(17), 10438-10447.